lajss.org
Latin American Journal of Solids and Structures
www.lajss.org

A-basis and b-basis buckling allowables for an aircraft composite wing

Roberto A. S. Cardoso[a*] ORCID 0009-0008-6779-2088, Marina S. Reis[b] ORCID 0009-0002-4474-3896, Leonardo P. S. Ferreira[c] ORCID 0000-0002-4963-8801, Mariana P. Alves[d] ORCID 0000-0002-8461-256X, Carlos A. Cimini Jr[e]. ORCID 0000-0002-6612-0211, Sung K. Ha[f] ORCID 0000-0002-4657-8727

[a] Federal University of Minas Gerais, Brazil, eng.robertocardoso@gmail.com
[b] Federal University of Minas Gerais, Brazil, marinasalesr@gmail.com
[c] FEMTO-ST, Applied Mechanics Department, France, leonardopsferreira@gmail.com
[d] Federal University of Minas Gerais, Brazil, maripimenta8@gmail.com
[e] Federal University of Minas Gerais, Brazil, carlos.cimini@gmail.com
[f] Hanyang University Seongdong-gu, Seoul, Korea, sungha@hanyang.ac.kr

* Corresponding author

Abstract
Buckling is a critical failure mode for aircraft composite panels. Therefore, determining the critical buckling load is essential for properly modeling. To optimize composite laminate structures, it is important to know the strength of the laminate, which can be obtained through statistical analyses based on test data. The resultant strength value is known as a design allowable. This paper aims to establish an approach to evaluate two types of statistically determined buckling allowables, A-Basis and B-Basis, for an aircraft composite wing. In this study, a finite element model of a composite semi-wing was used to perform linear buckling simulations. Six input parameters were initially selected as relevant to affect the buckling strength of the semi-wing: four material properties and two geometric parameters. A set of Monte Carlo simulations was conducted varying these parameters of interest, followed by a global sensitivity analysis using Sobol indices to identify the influence of each one, individually (first-order) and in pairs (second-order). A surrogate model based on artificial neural networks was then trained using data from the Monte Carlo simulations. Finally, this surrogate model was used to define the A-Basis and B-Basis allowables for a critical loading case.

Keywords
Linear buckling strength; Design allowables; Sensitivity analysis; Sobol indices; Surrogate models

Graphical Abstract

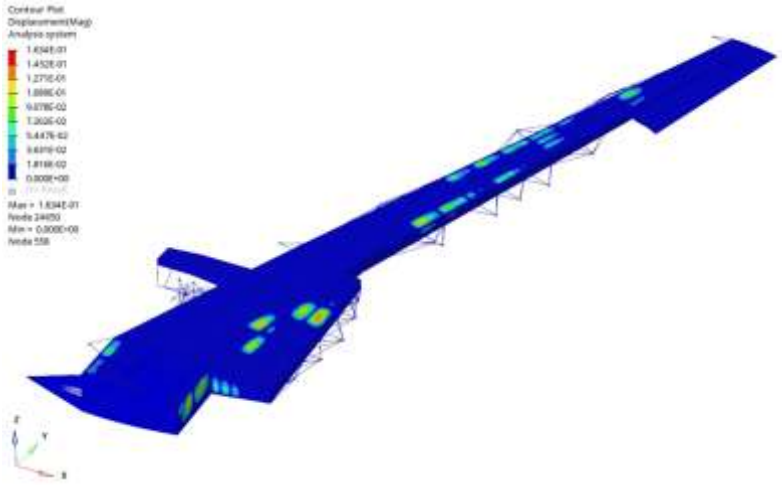

1 INTRODUCTION

The number of aircraft projects with composite materials has been continuously increasing in the last decades. Initially, the same project techniques employed in metallic materials were also applied to composites. However, the development of specific methods applicable to composite materials evolved to improved designs (Harris et al., 2002; Baker at al., 2002; Kennedy and Martins, 2012). During the design phase of an aeronautical component, statistical analyses are applied to define the component strength, resulting in design allowables (Nettles, 1994). Statistically determined allowables are divided into two types: A-Basis and B-Basis (MIL-HDBK-17-1F, 2002). A-Basis refers to the value in which only 1% of the population can fail, while B-Basis is the value in which 10% of the population have a possibility of failing, both considering a confidence level of 95%.

Among possible failures affecting aeronautical components, buckling is a mode that can be briefly defined as the loss of stability of a structure under shear and/or compression loads. Therefore, defining the A-Basis and B-Basis buckling allowables of aircraft composite panels under bending and torsion is an important step during the design process.

Enhancing and automating the processes related to the determination of the critical buckling load is relevant in the development of better modeling techniques for composite laminates. Machine learning algorithms can be used to speed up the process of designing a component, due to their ability of learning and processing large amounts of data. Artificial neural networks (ANNs) are a type of feedforward neural networks that can be used as surrogate models and perform the role of interpolators within the range of the training data. Previous works used neural networks as surrogate models for applications such as aerodynamics (Sun and Wang, 2019), optimization (White et al., 2019), and Lamb wave propagation (Ferreira et al., 2024) in composite materials.

The objective of this work is to define the A-Basis and B-Basis linear buckling design allowables for bending/torsion of a composite semi-wing through a surrogate model generated by finite element (FE) and ANN analyses. In the process, the main parameters of importance for the linear buckling strength were also obtained.

2 THEORETICAL BACKGROUND

The framework to develop this work is depicted in Figure 1. The FE model obtained from Silva et al. (2019) was submitted to a critical load case considering adequate boundary conditions. Linear buckling analyses (eigenvalues) were performed using the FE platform HyperMesh® with MSC NASTRAN®. Critical parameters related to the material and the geometry were initially selected as potentially important for buckling strength analyses. These parameters had their values defined through a random generation process (Monte Carlo simulations), bounded by realistic experimental coefficients of variation (CVs) obtained from Marlett et al. (2011). Monte Carlo simulations using the same FE model generated a data set of output responses (eigenvalues for linear buckling) based on the uncertainties of the input parameters. The results were then submitted to a global sensitivity analysis using Sobol Indices (first- and second-order), to identify the main parameters of influence. Finally, an Artificial Neural Network (ANN) was trained with the generated data set and the results of convergence between a surrogate model and the FE model were validated, leading to the use of this metamodel to statistically define the A-Basis and B-Basis buckling allowables.

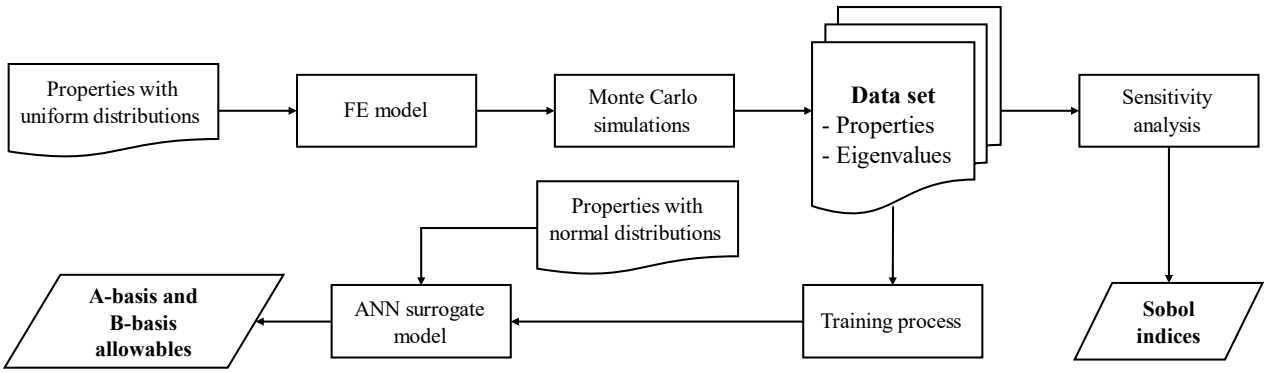

Figure 1 *– Proposed framework.*

The following subsections discuss relevant background topics related to the proposed framework.

2.1 Sobol indices

A sensitivity analysis aims to evaluate the impact of input parameters' variations on a model's output. This is performed through the identification of metrics that represent the output and through the qualification of the influence of each parameter on these metrics (Hornik et al., 1989). Assuming a numerical model in the form of:

$$Y = \mathcal{M}(\Theta) \tag{1}$$

where $\Theta = (\theta_1, \theta_2, \dots, \theta_k)$ is a vector comprising k input parameters and Y is a scalar quantity that represents the output of the numerical model. The global sensitivity analysis using Sobol indices decomposes the model's response Y in terms increasing dimensions:

$$Y = \mathcal{M}_0 + \sum_{i=1}^{k} \mathcal{M}_i(\theta_i) + \sum_{i<j}^{k} \mathcal{M}_{ij}(\theta_i, \theta_j) + \cdots + \mathcal{M}_{1\dots k}(\theta_1, \dots, \theta_k) \tag{2}$$

where the constant $\mathcal{M}_0$ corresponds to the expected value $E(Y)$ of the model output, and $\mathcal{M}_i(\theta_i)$ and $\mathcal{M}_{ij}(\theta_i, \theta_j)$ are the conditional means for parameters i and j $(i \neq j)$, defined as:

$$\mathcal{M}_i(\theta_i) = \int_0^1 \dots \int_0^1 \mathcal{M}(\boldsymbol{\theta})\, \mathrm{d}\boldsymbol{\theta}_{\sim i} - \mathcal{M} \tag{3}$$

$$\mathcal{M}_{ij}(\theta_i, \theta_j) = \int_0^1 \dots \int_0^1 \mathcal{M}(\boldsymbol{\theta})\, \mathrm{d}\boldsymbol{\theta}_{\sim ij} - \mathcal{M}_0 - \mathcal{M}_i(\theta_i) - \mathcal{M}_j(\theta_j) \tag{4}$$

where the notation $\sim i$ indicates that the parameter θ_i is excluded. As the model response from Eq. (1) is also a random variable, the conditionals can be considered a measure of the model output variance. Therefore, the first-order Sobol indices can be computed as:

$$S_i = \frac{Var[\mathcal{M}_i(\theta_i)]}{Var[\mathcal{M}(\boldsymbol{\theta})]} \tag{5}$$

The second-order Sobol indices can be defined as:

$$S_{ij} = \frac{Var\left[\mathcal{M}_{ij}(\theta_i,\ \theta_j\ )\right]}{Var[\mathcal{M}(\boldsymbol{\theta})]} \tag{6}$$

These indices quantify the individual effect of each parameter and the pair-like combination of two parameters in the model's output, respectively.

2.2 Neutral networks

A neural network is a computational model designed to recognize patterns and make predictions by mimicking the structure and function of neurons. The most used neural network type is the multilayer perceptron (MLP) due to its ease of implementation and robustness. MLP networks consist of a series of interconnected layers of neurons in which one layer receives the information from the previous layer, processes it, and then forwards it to the next layer.

Assuming a training dataset with dimension $M \times N$, where M is the number of points per array, and N is the number of samples in the dataset, the l-th sample vector is represented by $x^{(l)} \in \mathbb{R}^{M \times 1}$. In a supervised learning scheme, the expected output for a training sample is represented by $y^{(l)} \in \mathbb{R}^{P \times 1}$, where P is the number of outputs. The objective of the neural network is to map the function $\mathcal{F}: x^{(l)} \rightarrow y^{(l)}$.

A neural network with at least one hidden layer can act as a universal approximator (Hornik et al. 1989). Each neuron in a hidden layer performs part of this mapping in the form:

$$x_{i+1,k} = G\left(\sum_{j=1}^{m} w_{ij,k} x_{ij} + b_{i,j}\right) \tag{7}$$

Considering the k^{th} unit (or neuron) of the i^{th} layer, it receives the output x_{ij} from each j^{th} unit of the $(i-1)^{th}$ layer. The values x_{ij} are then multiplied by a weight w_{ij}, and these products are added. A bias $b_{i,j}$ is added to the result, and then an activation function G is applied to the result that is propagated to the next layer. The activation function is responsible for adding non-linearity to the system, and it can assume multiple forms, from Rectified Linear Unit (ReLU) and leaky ReLU functions to sigmoid functions, e.g., logistic function and hyperbolic tangent ($tanh$).

2.3 A-Basis and B-Basis design allowables

The use of an allowable mechanical property has the goal of safe design through conservative values of material properties with a high level of reliability. According to the MIL-HDBK-17 (2002), considering a normal distribution, both

A-Basis and B-Basis design allowables are obtained for a 95% confidence level on the statistical analysis. As mentioned before, A-Basis is restricted to the 1st percentile while B-Basis is relaxed to the 10th percentile (Figure 2).

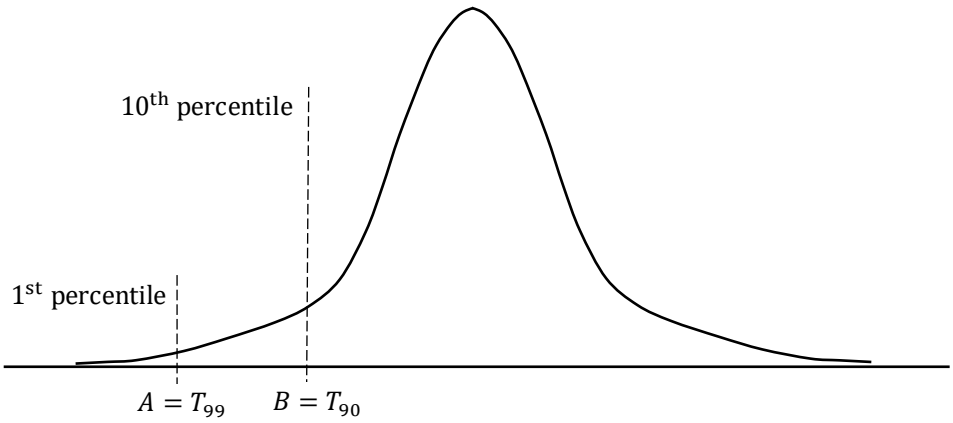

Figure 2 *– Limits for A-Basis and B-Basis design allowables in a normal distribution curve.*

When it comes to a population following a normal distribution, A-Basis and B-Basis values can be calculated using the following equations:

$$\mathrm{A_{Basis}} = \mu * k_A \sigma \quad (8)$$

$$\mathrm{B_{Basis}} = \mu * k_B \sigma \quad (9)$$

where μ is the mean of the population values, k_A and k_B are one-side limit factors that depend on the number of samples n, and σ is the standard deviation. The one-side limits can be defined as:

$$k_A \approx 2.3226 + e^{1.34 - 0.520 \ln(n) + \frac{3.87}{n}} \quad (10)$$

$$k_B \approx 1.282 + e^{0.958 - 0.520 \ln(n) + \frac{3.19}{n}} \quad (11)$$

3 METHODOLOGIES

3.1 Selected material and parameters of influence

The selected material system was AS4/8552 (CFRP), with properties obtained from Marlett et al. (2011). The unidirectional ply was set as the building block for the stacking sequence of the laminates. In order to verify the influence of the input uncertainties in the output design, six parameters of interest were selected:

- E_1, Young's modulus in the direction of the fibers;
- E_2, Young's modulus in the direction perpendicular to the fibers;
- G_{12}, in-plane shear modulus;
- ν_{12}, major Poisson's ratio;
- α, ply angle, and
- t, ply thickness.

The first four parameters are the engineering constants of the material system and the last two parameters are related to the ply geometry. All uncertainties (mean and standard deviation) for each parameter were obtained from the experimental work in Marlett et al. (2011), except the ply angle α which was considered to vary from –2° to +2° in every ply.

3.2 Software

A model of the composite semi-wing (Silva et al., 2019) was implemented using HyperMesh® as pre- and post-processor, while NASA Structural Analysis (NASTRAN®) was used as the solver for all structural analyses. The model was automated to generate Monte Carlo sets using an algorithm implemented in Microsoft Excel® Visual Basic for Applications (VBA) that generates input cards, while NASTRAN® runs the simulations, creating a file that is read by the VBA script and added to a MS Excel® spreadsheet. Finally, the statistical analyses were performed using MATLAB® and UQLab® framework extensions.

3.3 Finite element model

The finite element model used in this work was obtained from Silva et al. (2019). It represents a semi-wing of a typical regional jet, as shown in Figure 3, which also depicts the FE mesh modeled with NASTRAN® composite shell element type PCOMP. This model was previously optimized through the slice and swap method resulting in several different layups for different patches colored in Figure 3 (Silva et al., 2019).

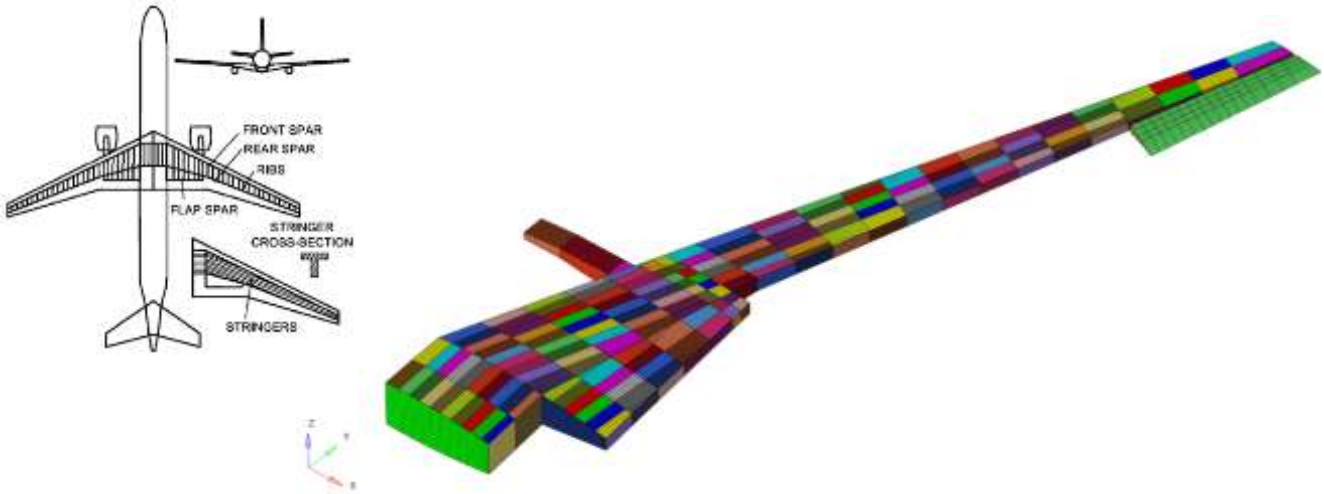

Figure 3 *– Finite element model mesh and layup patch optimization (Silva et al., 2019).*

The layups considered the use of QUAD legacy (four angles: 0°, +45°, –45°, and 90°) and followed the aeronautical industry design rules (Silva et al., 2019):

Symmetry: Stacking sequences must be symmetric about the midplane.

Balance: Stacking sequences should have the same number of $+\vartheta$ and $-\vartheta$ plies.

Contiguity: No more than three plies of the same orientation may be stacked together.

Disorientation: Difference between orientations of two consecutive plies should be equal or less than 45°.

10% rule: A minimum of 10% of plies in each QUAD angle is required.

A critical loading case corresponding to a maximum load factor ($n_z = 2.5$) maneuver at cruising speed (Mach 0.82) with Maximum Take-Off Weight (MTOW) configuration at altitude of 10,000 m was considered for all simulations. Loading and boundary conditions (symmetry clamping at wing root) are depicted in Figure 4.

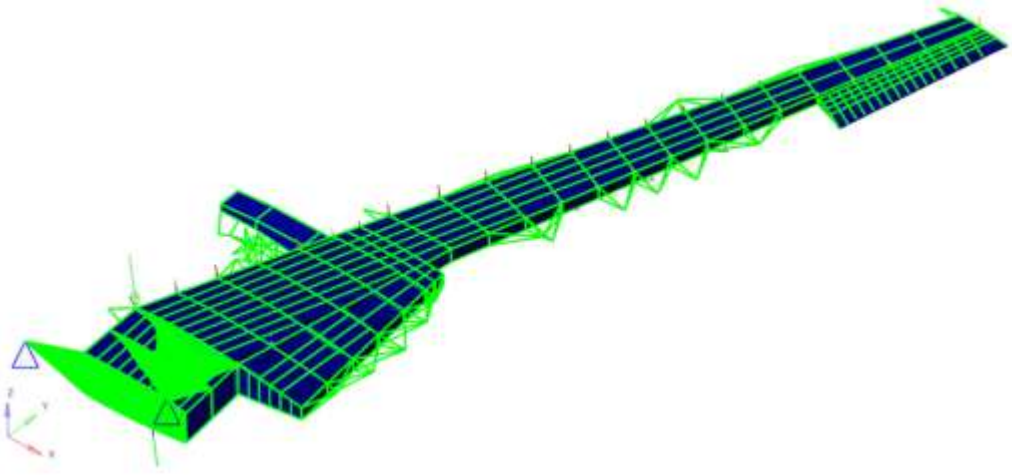

Figure 4 *– Loading and boundary conditions (Silva et al., 2019).*

Linear buckling analyses were performed determining the buckling strength of the composite semi-wing in terms of eigenvalues, correlated to the corresponding buckling mode shapes.

3.4 Monte Carlo simulation

To estimate the uncertainties in the linear buckling behavior, 1,000 sets of the six mechanical and geometrical parameters were randomly generated using a uniform distribution, in which all outcomes are equally likely. These Monte Carlo sets were based on uncertainty limits defined according to the mean (μ) and standard deviation (σ) values for the material system AS4/8552, experimentally obtained by Marlett et al. (2011).

In order to enhance the coverage of the experimental population, an extension of the uncertainties was expanded to 4 standard deviations (4σ), thus covering 99.9937% of the test data for each parameter (Figure 5). The parameters of interest are shown in Table 1, together with the mean, lower bound and upper bound values used in the Monte Carlo simulations, covering the range between $\mu - 4\sigma$ and $\mu + 4\sigma$. The ply angle variation $-2° \leq \alpha \leq +2°$ is simultaneously considered equal for all plies in the laminates. In other words, the angle α can be considered as a rigid-body rotation of the stacking sequence for all laminates in the semi-wing.

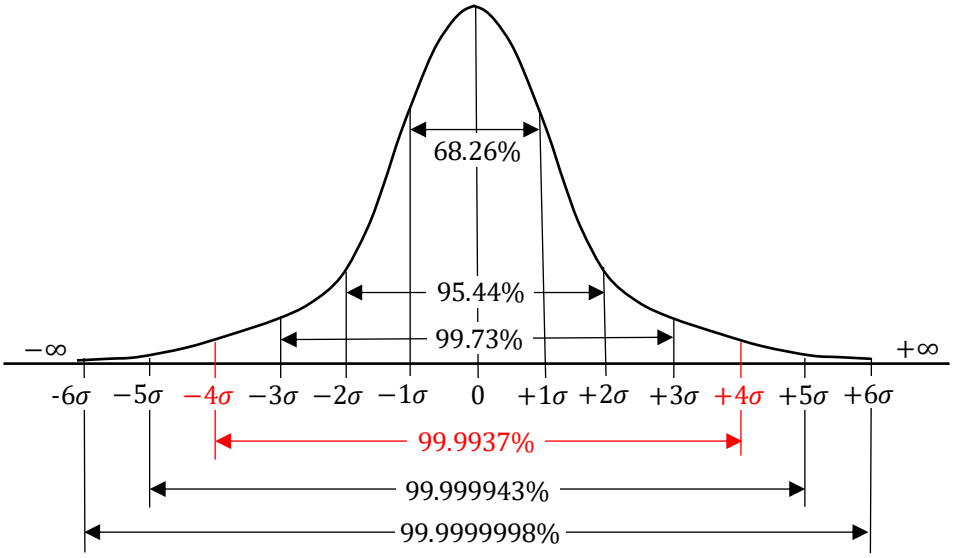

Figure 5 *– Population coverage as a function of the number of standard deviations in a normal distribution curve.*

Table 1 *– Parameters and bounds used for Monte Carlo simulation (Marlett et al., 2011).*

Parameter	Mean (μ)	Standard Deviation (σ)	4 Standard Deviations (4σ)	Lower Bound ($\mu - 4\sigma$)	Upper Bound ($\mu + 4\sigma$)
E_1	119 GPa	6.00 GPa	24.0 GPa	95.0 GPa	143 GPa
E_2	9.8 GPa	0.3 GPa	1.2 GPa	8.6 GPa	11 GPa
ν_{12}	0.316	0.038	0.153	0.163	0.469
G_{12}	4.7 GPa	0.15 GPa	0.60 GPa	4.1 GPa	5.3 GPa
α	–	–	–	$\alpha - 2°$	$\alpha + 2°$
t	0.186 mm	0.007 mm	0.028 mm	0.158 mm	0.214 mm

To automate the generation of data related to the different FE models performing the Monte Carlo linear buckling simulations, a spreadsheet containing all the information to be altered from the original model was created using MS Excel®. This document includes 1,000 random values for each one of the parameters of reference (E_1, E_2, G_{12}, ν_{12}, α, and t) within the defined boundaries. Using MS Excel® VBA, a script was developed to read the FE input files and rewrite them formatted with the modifications. Every new FE model generated was saved with a name corresponding to the randomly defined parameters. After automatically running the simulations of each FE case generated, the solver NASTRAN® outputted the data of the linear buckling simulation (eigenvalues and eigenvectors), and the VBA code automatically created a text file with the results, which were later added to a new column in the original spreadsheet (Figure 7). This data set file was then used to feed the sensitivity analysis and train the ANN to obtain the surrogate model.

3.5 Sensitivity analysis

Using the Monte Carlo data set generated and stored, a Sobol sensitivity analysis was conducted to verify the most influential input parameters in the linear buckling strength of the studied semi-wing. A first-order Sobol analysis was performed for individual parameters considered separately and followed by a second-order analysis which correlated pairs of parameters. Sobol indices were computed using MATLAB® and the UQLab® framework (Marelli and Sudret, 2014).

3.6 Surrogate model

As finite element simulations can be very time-consuming, it was proposed to use a surrogate model to replace the FE model for the A-basis and B-basis design allowables generation. Multiple techniques are available for surrogate modeling, such as the Gaussian process, Polynomial Chaos Expansion (PCE), or ANN. The selected surrogate model in this study was a multilayer perceptron ANN, used as an interpolation model inside the parameters' space available for simulating the numerical model.

The input layer consisted of 6 neurons, representing the random variables E_1, E_2, G_{12}, ν_{12}, α, and t, and the output layer had one neuron representing the eigenvalue for the linear buckling analysis. The number of hidden layers was defined as 2, with 80 and 120 neurons, respectively. The number of neurons in each layer was defined through a convergence analysis using the eigenvalue as metric and the number of neurons on each layer as input.

The data set generated from the Monte Carlo simulations was used to train the surrogate model. From the 1,000 Monte Carlo samples, 800 were used for training the ANN and 100 were used for verifying the convergence through a feedback process. The remaining 100 samples, not used in the processes of training and verification, were used to test the generated metamodel for accuracy.

As convergence and correlation were verified, the surrogate statistical model was used for the definition of the A-basis and B-basis buckling strength allowables.

4 RESULTS AND DISCUSSION

4.1 FE model deterministic results

Deterministic simulation was performed in the FE model using the mean values for the material and geometric parameters (Table 1) (Marlett et al., 2011). The eigenvalues for the first 10 linear buckling modes are listed in Table 2. The envelope of the 100 linear buckling modes is graphically depicted in Figure 6. The first buckling mode for which the semi-wing was optimized is defined as the linear buckling strength.

Table 2 *– Eigenvalues for the 10 first linear buckling loads of the semi-wing FE model.*

Buckling mode	Eigenvalue
1st	1.0000000
2nd	1.0232411
3rd	1.0351196
4th	1.0925866
5th	1.1486894
6th	1.1597451
7th	1.1785044
8th	1.2111119
9th	1.2177263
10th	1.2212535

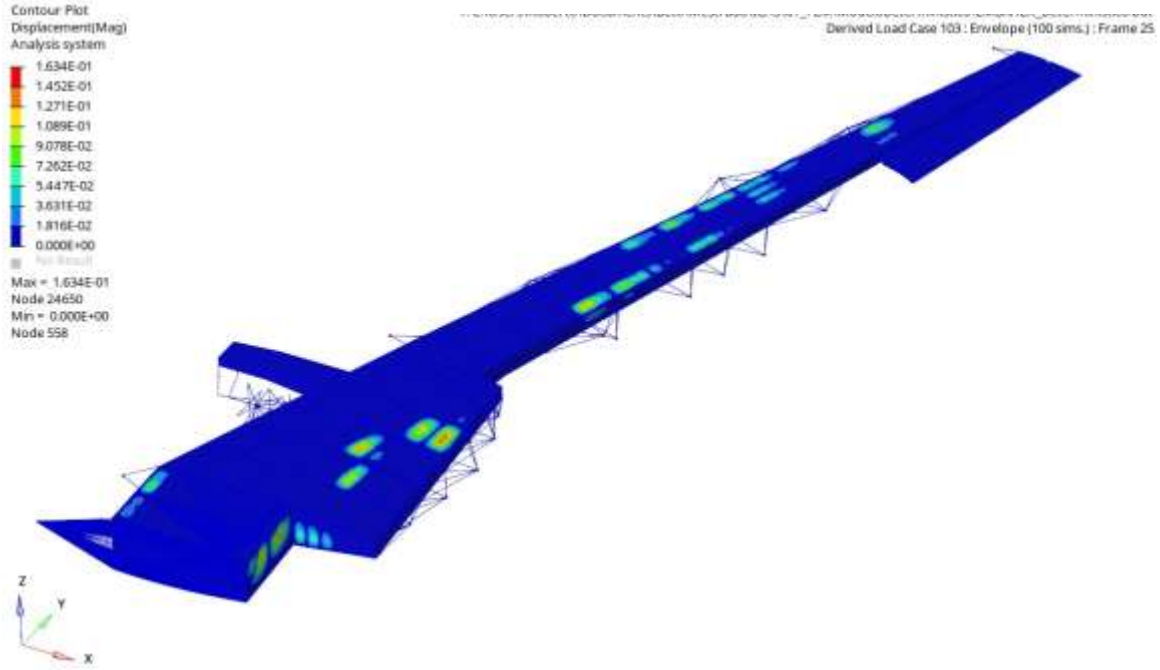

Figure 6 *– Envelope of the first 100 linear buckling modes.*

4.2 Monte Carlo results

Monte Carlo simulations were performed using the FE model for different input sets randomly varying the 6 parameters of interest. A spreadsheet was generated with 1,000 lines containing different values of the input variables E_1, E_2, G_{12}, ν_{12}, α, and t, and the respective eigenvalue for each input set. A schematic snapshot of the spreadsheet is shown in Figure 7.

Run	E1 [MPa]	E2 [MPa]	G12 [MPa]	NU12	Alpha [°]	Ply Tck [mm]	Eigenvalue
1	100775.0	10807.0	4571.0	0.431	-1.9	0.164	0.6583685
2	108573.0	10008.0	4856.0	0.427	-0.6	0.158	0.6331974
3	97638.0	9907.0	4657.0	0.170	0.2	0.184	0.8676227
4	136659.0	8813.0	4124.0	0.408	-1.8	0.193	1.1741304
5	114259.0	9273.0	4394.0	0.436	-0.4	0.168	0.7674372
...	...	...	...	...	...	...	...
1000	137733.0	8788.0	4468.0	0.42	0.0	0.210	1.3261949

Figure 7 *– Schematic snapshot of the spreadsheet with data from the Monte Carlo simulations.*

4.3 Sensitivity analysis results

Figure 8 presents the results obtained from the sensitivity analysis. Since UQLab uses an interpolation model based on Polynomial Chaos Expansion (PCE) during the calculation of Sobol indices, multiple tests were performed to evaluate the convergence of the resultant indices. For this purpose, 200 samples from the Monte Carlo simulations were set aside as a validation set, and different amounts of samples were used to evaluate the evolution of error in the PCE definition. Figure 8a shows the evolution of the PCE error in the validation set with respect to the number of samples. Note that the error decreases rapidly with fewer than 100 samples and continues to decrease until stabilizing near 0.2% with 600 samples. Figure 8b shows the evolution of the Sobol indices for multiple parameters concerning the number of samples. The Sobol indices stabilize after approximately 400 samples. Therefore, convergence is ensured using the available 800 samples in the calculation of the Sobol indices.

Figure 8c depicts the first-order Sobol indices obtained using 800 samples. The main parameters affecting the eigenvalue's results are the thickness of the layers, t, and the longitudinal modulus of elasticity in the fiber direction, E_1, with Sobol indices of 0.9 and 0.1, respectively. The remaining parameters have negligible influence on the model's output variance. Given that the sum of first- and second-order Sobol indices adds to one, the second-order indices are null, indicating that interactions between two distinct parameters also do not present a measurable influence on the eigenvalues

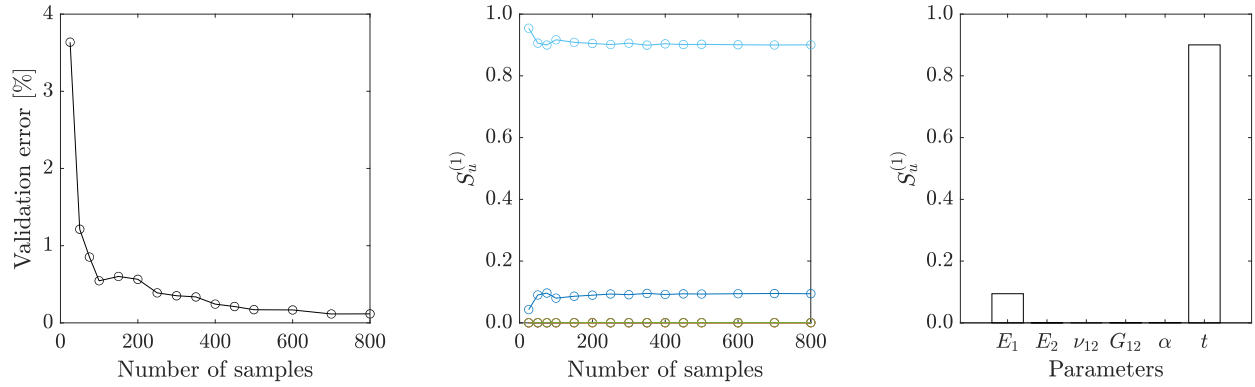

(a) (b) (c)

Figure 8 *– Results from the sensitivity analysis: (a) convergence of PCE error, (b) convergence of Sobol indices concerning number of samples, and (c) first-order Sobol indices*

4.4 Surrogate model

After concluding the global sensitivity analysis, a surrogate model was developed to replace the FE model in the calculation of allowables, considering 99.9937% of the expected values for the experimental properties, assuming a normal distribution (4σ). The proportion of 8/1/1, i.e., 800 samples for training, 100 for validation, and 100 for testing was used for the ANN. The input parameters were normalized between 0 and 1, and the output eigenvalues were normalized between -1 and 1 to improve convergence. The network was trained using the Adam optimization algorithm with a learning rate of 0.005 and a convergence criterion based on the stabilization of the error on validation data was implemented. The test data was used only after the training and selection of the final network to evaluate its performance on unseen data. Figures 9(a) to 9(c) compare the predictions for the eigenvalues for the FE model and the surrogate mode, while Figures. 9(d) to 9(f) present the error distribution of the surrogate model for the training, validation and test subsets.

The results on training, validation and test data show that the surrogate model can predict eigenvalues in line with the results obtained from the FE model. Evaluating the cumulative density function in the error curves, 90% of the results in training, validation and test of the ANN are below 2% error, and 99% of the results present less than 3.5% error when compared to the FE model's results. These values represent an adequacy between the models. Regarding the training data, during the training process, some values did not follow the linearity expected which led to a higher error percentage in this data set, although it can still be considered acceptable in the broader aspect of the analyses.

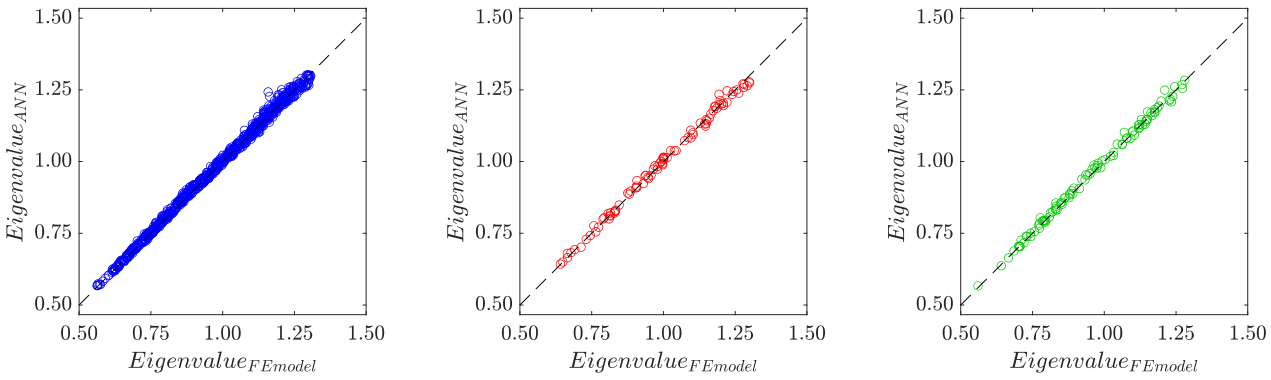

(a) (b) (c)

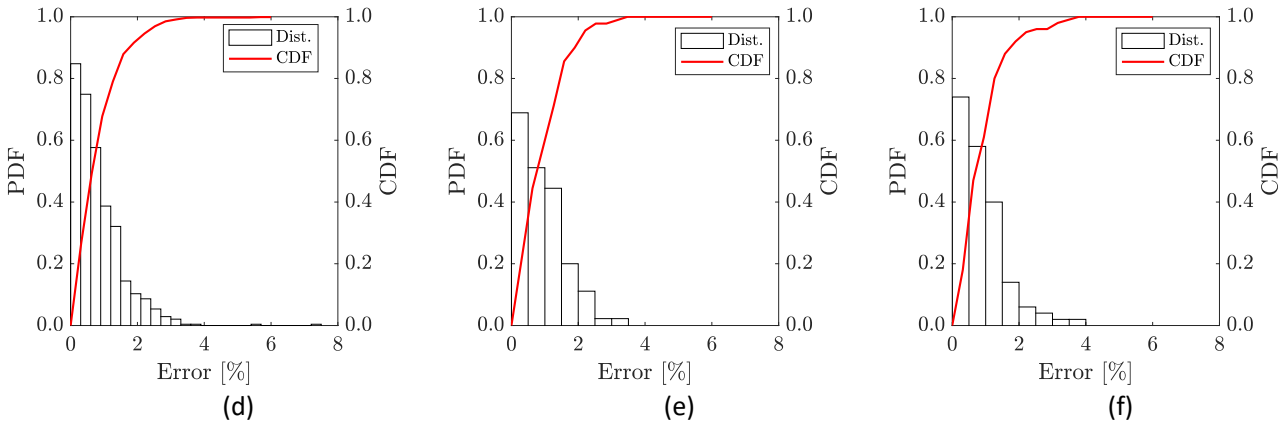

Figure 9 *– Error evaluation for the surrogate model. Eigenvalues comparison for the FE model and ANN using (a) training, (b) validation, and (c) test data, and error distribution for (d) training, (e) validation and (f) test data.*

The primary advantage of the surrogate model is its computational efficiency. After the training phase, a batch of 1,000 evaluations takes less than 0.01 seconds, compared to approximately 30 hours for the same number of simulations using the FE model. This efficiency enables the surrogate model to be evaluated under various conditions within its training boundaries, allowing for the assessment of the impact of mechanical property variations on the eigenvalues.

4.5 Allowables

For the calculation of allowables, the mechanical properties and ply thickness for the material system AS4/8552 (Table 1) were employed to sample normal distributions. Each mechanical property and ply thickness parameter was considered to follow a normal distribution, with the mean values centered at the nominal value. Furthermore, the angle orientation of each ply layer was also assumed to follow a normal distribution centered at its nominal value and with 4σ spanning $\pm 2°$. This approach accounts for realistic manufacturing variations and ensures that the surrogate model remains inside its training boundaries. A total of 10,000 samples were generated for each property and used as input for the surrogate model. All properties are presented in Figures. 10(a) to 10(f).

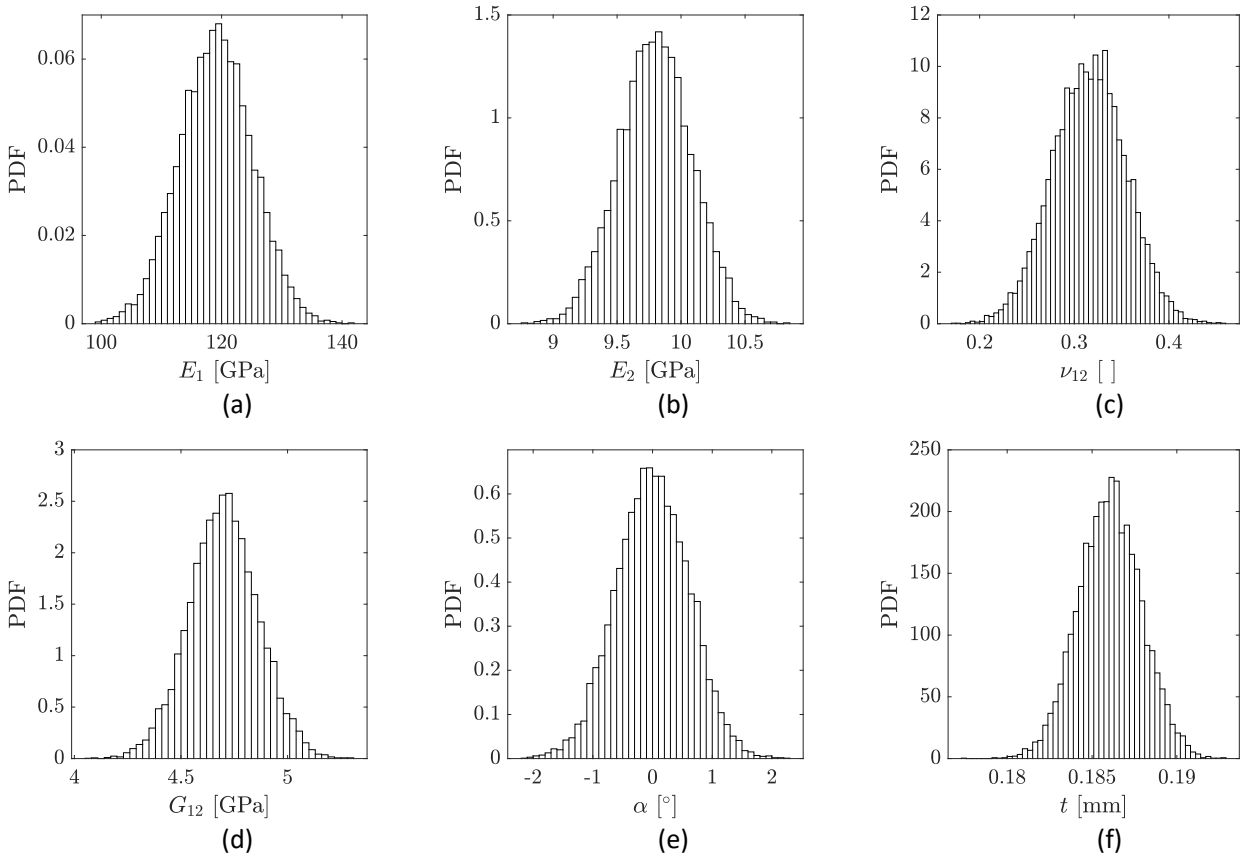

Figure 10 *– Properties distribution used for allowables calculation.*

Figure 11 presents the eigenvalues obtained using the surrogate model based on properties from Figure 10. The model predicts the A-basis and B-basis eigenvalues of the structure as 0.914 and 0.952, respectively. These predictions are made within the known margin of error of 3.5% in a worst-case scenario, as detailed in Section 4.4. The mean for the eigenvalue is 0.996, which corresponds to the mean value for the distributions and is in line with the optimized eigenvalue from Table 2.

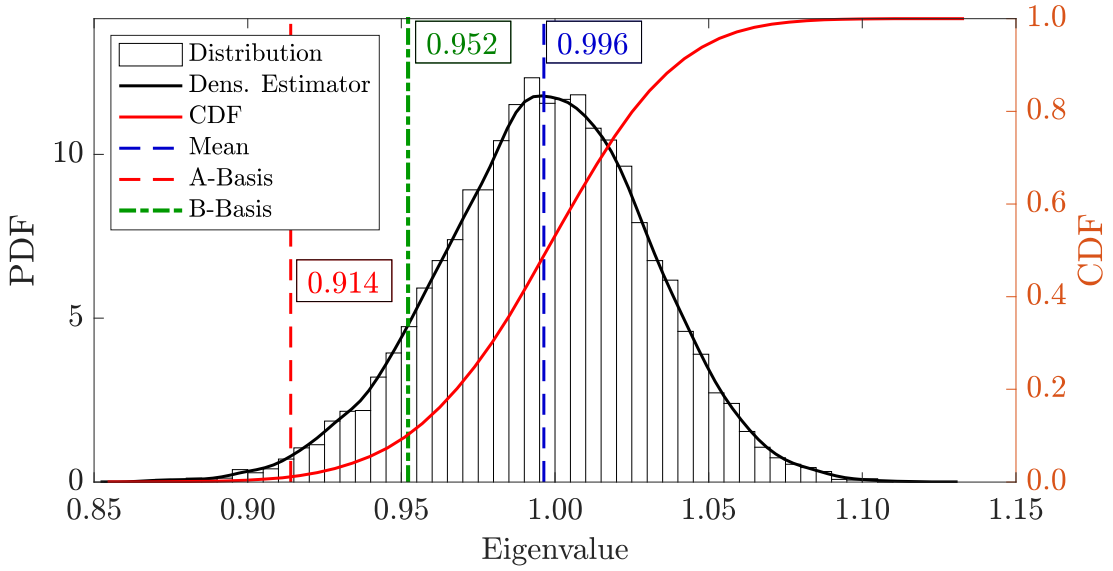

Figure 11 *– Eigenvalues distribution and estimative for A-basis, B-basis and mean value.*

The surrogate model demonstrates computational efficiency by simulating the proposed 10,000 samples in less than one second, a task that would take the FE model over a week to complete. This capability allows extensive parametric studies and reliability assessments by varying the mechanical properties of the composite material inside the training span of the model. Additionally, the proposed strategy is adaptable to other structural models and can be extended to encompass a broader range of properties. This flexibility allows designers to evaluate multiple conditions of material properties efficiently.

The main cost associated with the surrogate model is the initial dataset used for training. Once trained, the model can function as an interpolator, replacing the FE model for subsequent analyses. This reduces computational time and resources while maintaining accuracy in predictions.

5 CONCLUSIONS

In this work, a finite element model of a composite semi-wing was simulated for different combinations of geometric and material parameters. The analyses were performed to verify the influence of the input parameters in the output eigenvalues results for linear buckling modes and to determine the A-Basis and B-Basis linear buckling allowables using a surrogate model.

The Sobol sensitivity analysis showed that the parameters influencing the most the final outputs were the thickness of the layers, t, and the longitudinal modulus of elasticity in the fiber direction, E_1. This information allows to properly direct efforts in the material tests, model development, and quality control, ensuring that these parameters are well addressed. Moreover, it was clear that the surrogate model considerably accelerates the development time once its computational cost is lower than the one of a FE model simulation. In this sense, it can be used to efficiently test combinations of parameters with a known error. In the present work, the error obtained was less than 2% for 90% of the samples.

Therefore, based on the results, using a surrogate model and an ANN to predict linear buckling allowables is a valid method that enhances and facilitates the design process. For the model of the composite semi-wing used, the resultant A-Basis and B-Basis allowables were 0.914 and 0.952, respectively, which are in accordance with the expected values.

ACKNOWLEDGEMENTS

Authors would like to acknowledge support from CNPq, CAPES and FAPEMIG. This publication was elaborated under the context of the Project ATED – Design Enabled by Aeroelastic Tailoring, developed in cooperation with Hanyang University, Federal University of Minas Gerais and Embraer.

Author's Contributions: Conceptualization, RAS Cardoso, LPS Ferreira and CA Cimini Junior; Methodology, RAS Cardoso, MS Reis, LPS Ferreira, MP Alves and CA Cimini Junior; Writing—original draft preparation, RAS Cardoso, MS Reis and LPS Ferreira; Writing—review and editing, RAS Cardoso, MS Reis, LPS Ferreira, MP Alves and CA Cimini Junior; Supervision, CA Cimini Junior and SK Ha; Funding acquisition, CA Cimini Junior and SK Ha. All authors have read and agreed to the published version of the manuscript.

Editor: Pablo Andrés Muñoz Rojas

References

Baker AA, Callus PJ, Georgiadis S, Falzon PJ, Dutton SE, Leong KH, (2002). An affordable methodology for replacing aircraft panels with advanced composites. Composites Part A, Vol. 33, pp. 687-696.

Ferreira LPS, Teloli RO, Silva S, Figueiredo E, Moldovan ID, Maia N and Cimini Jr CA, (2024). Bayesian calibration for Lamb wave propagation on a composite plate using a machine learning surrogate model. Mechanical Systems and Signal Processing, Vol. 208, paper 111011, pp 1-16.

Harris CEH, Starnes Jr JHS, Shuart, MJ, (2002). Design and manufacturing of aerospace composite structures, State-of-the-art assessment. Journal of Aircraft, Vol. 39, No. 4, pp. 545-560.

Hornik K, Stinchcombe M, White H, (1989). Multilayer feedforward networks are universal approximators. Neural Networks, Vol. 2, pp. 359-366.

Kennedy GJ, Martins JRRA, (2012). A comparison of metallic and composite aircraft wings using aerostructural design optimization. Procedures of the 12th AIAA Aviation Technology, Integration, and Operations (ATIO) Conference and 14th AIAA/ISSM 17, paper AIAA 2012-5475, Vol.1, pp 1-31.

Marelli S, Sudret B, (2014). UQLab: A framework for uncertainty qualification in Matlab. Vulnerability, Uncertainty, and Risk, ASCE, Vol.1, pp 2554-2563, 2014.

Marlett K, Ng Y, Tomblin J, Hooper E, (2011). NCAMP Test Report: CAMP-RP-2010-002 Rev A. Hexcel 8552 AS4 Unidirectional Prepreg at 190 gsm & 35% RC Qualification Material Property Data Report, Technical Report, National Institute for Aviation Research.

MIL-HDBK-17-1F, (2002). Polymer matrix composites guidelines for characterization of structural materials. Vol. 1, U.S. Department of Defense.

Nettles A, (1994). Allowables for structural composites. Proceedings of the International Conference on Composites Engineering, Vol.1, pp 1-2.

Silva GHC, Prado AP, Cabral PH, De Breuker R, Dillinger JKS, (2019). Tailoring of a composite regional jet wing using the slice and swap method. Journal of Aircraft, Vol. 56, No. 3, pp 1-15.

Sun G, Wang S, (2019). A review of the artificial neural network surrogate modeling in aerodynamic design. Proceedings of the Institution of Mechanical Engineers, Part G: Journal of Aerospace Engineering, Vol. 233, No. 16, pp 5863-5872.

White DA, Arrighi WJ, Kudo J, Watts SE, (2019). Multiscale topology optimization using neural network surrogate models. Computer Methods in Applied Mechanics and Engineering, Vol. 346, pp 1118-1135.